Impact Response of Torsionally Coupled Base-isolated Structures

V A Matsagar and R S Jangid

Journal of Vibration and Control published online 9 April 2010
DOI: 10.1177/1077546309103271

Journal of Vibration and Control OnlineFirst, published on April 9, 2010 as doi:10.1177/1077546309103271

Impact Response of Torsionally Coupled Base-isolated Structures

V. A. MATSAGAR
R. S. JANGID
Department of Civil Engineering, Indian Institute of Technology Bombay, Powai, Mumbai – 400 076 (India) (rsjangid@civil.iiitb.ac.in)

(Received 21 June 2008; accepted 16 October 2008)

Abstract: The seismic response of a single-story asymmetric structure supported on various base isolation systems during impact with adjacent structures is investigated. Eccentricities arising due to elastic forces in the columns at the top-deck and the restoring forces in the isolation systems at the base-raft are considered. The adjacent structures (i.e. retaining walls or entry bridges) surrounding the base-isolated structure on all four sides are modeled in the form of springs and dashpots. The coupled differential equations of motion for the isolated system are derived and solved in incremental form using Newmark's method to obtain the seismic response with and without impact. The variation of superstructure acceleration and isolation level displacement during impact upon the adjacent structures under the action of real earthquakes are computed to study the behavior of torsionally coupled structures and compare the performance of various isolation systems. The torsional impact response of isolated structures is studied under the variation of important system parameters such as the sizes of gaps, the stiffness of adjacent structures, superstructure flexibility and different eccentricities in the base-isolated structure. It is concluded that the lateral-torsional response of the base-isolated structure is adversely affected when impact takes place with the adjacent structures. The superstructure acceleration increases and the base-raft displacement decreases due to impact with the adjacent structures; nevertheless, the isolation remains effective as compared to the nonisolated case. Further, it is also observed that superstructure acceleration increases with increase of the isolation gap distances up to a certain value and then the acceleration decreases with its further increase. The effects of impact are found to be severe for systems with flexible superstructure, stiffer adjacent structures and increased eccentricities.

Key words: Structure, asymmetry, isolation, impact.

1. INTRODUCTION

The base isolation technique is an aseismic design approach in which, due to the insertion of a flexible layer between the foundation and the superstructure, the fundamental frequency of the system decreases to a value lower than the predominant energy-containing frequencies of earthquake ground motions. In addition, the damping capacities provided by the isolation systems help dissipate the energy imparted during seismic activities. Thus, the isolation becomes an attractive approach to safeguard the structures against earthquakes without any requirement for modification in the superstructure. A variety of isolation systems have been

 DOI: 10.1177/1077546309103271

Figures 4–16 appear in color online: http://jvc.sagepub.com

developed and used for aseismic design of structures (Kelly, 1986; Buckle and Mayes, 1990; Jangid and Datta, 1995). However, with the addition of a flexible layer at the foundation, i.e. at isolation level, the peak displacements across it increase significantly during earthquakes and the structure may collide with adjacent structures such as boundary retaining walls, entrance ramps etc. if the separation gap distance is inadequate. Further, in buildings with longer plan dimensions, expansion gaps are provided to accommodate the displacements arising due to temperature variations. At these gaps, there are chances that impact will occur when the two building units vibrate out of phase during earthquakes. Such incidence of impact in base-isolated buildings was reported during the 1994 Northridge earthquake, reducing the effectiveness of isolation (Nagarajaiah and Sun, 2001). The impact problem in the case of a base-isolated structure has been studied by Maison and Ventura (1992), Hall et al. (1995), Malhotra (1997) and Tsai (1997). The severity of impact in the case of base-isolated buildings and the comparative performance of various isolation systems has been studied by Matsagar and Jangid (2003) for a shear model of the structure, dealing with two-dimensional (2D) idealization; wherein the impact considered was in the normal direction (not oblique) as no rotational degrees-of-freedom were considered. However, such 2D modeling leads to unrealistic results for the structures with asymmetric plans, and therefore a three-dimensional (3D) analysis of such systems is highly essential to obtain the accurate design displacements and forces (Tsopelas et al., 1994; Tena-Colunga and Gomez-Soberon, 2002). Most of the real structures are asymmetrical because of their mass and/or stiffness distributions, contrary to an ideal 2D system. The structural irregularities such as irregular distribution of mass, stiffness or strength in their floor plan leads to coupling of responses in the lateral and torsional directions. The structures excited by earthquake ground motions undergo lateral as well as torsional motions if the centers of structural mass and stiffness do not coincide at the floor level. Such a torsional coupling in the case of base-isolated structures may lead to a substantial increase in seismic response, which essentially depends upon properties of the structure and the isolation system utilized. As the bearings are essentially isotropic in nature, the same natural frequencies occur in the lateral and longitudinal directions of the system. However, when the structure is torsionally coupled due to dissimilarity of the different bearing parameters or the system properties, a strong coupling of responses in the three principal directions may occur when the torsional frequency is closer to the two lateral frequencies. Such torsional coupling occurs, especially in the case of base-isolated structures, if the eccentricity between the center of mass (CM) and the center of rigidity (CR) exists at the superstructure and/or the isolation levels (Matsagar and Jangid, 2005). The structure may experience a highly increased response when the line joining the CM and the CR is perpendicular to the direction of earthquake excitation. Therefore, it will be interesting to study the dynamic behavior of flexible single-story structures supported on different isolation systems during impact with the adjacent structures.

In this paper, the impact response of asymmetric base-isolated single-story structures is investigated under different real earthquake ground motions. The eccentricities arising due to dissimilar isolator parameters are duly formulated. The specific objectives are to study: (i) the performance of different isolation systems during torsional impact; (ii) the influence of variation in parameters of the base-isolated structures such as flexibility of the superstructure and eccentricities on the impact response; and (iii) effects of variation in the properties of the adjacent structures such as stiffness and separation gap distances on the torsional impact response.

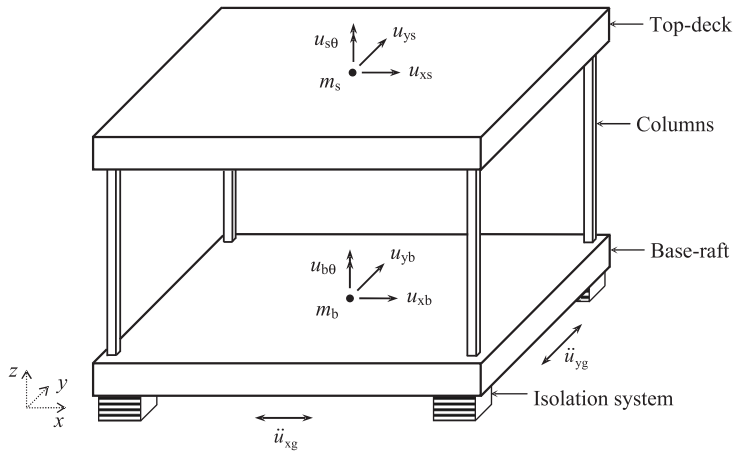

Figure 1. Mathematical model of a single-story asymmetric isolated structure.

2. MODELING OF ISOLATED AND ADJACENT STRUCTURES

Figure 1 shows the idealized mathematical model of an asymmetric single-story base-isolated structure considered in the present study. The top-deck of dimensions $B \times D$ in the plan is supported by massless, axially inextensible columns. The base-raft of dimensions $B \times D$ in the plan is mounted on various types of seismic isolators. The CR of the columns may not coincide with the CM of the top-deck, and the CR provided by the restoring forces in the isolation systems at the base-raft may not coincide with the CM of the base-raft as shown in Figure 2. Hence, the main sources of asymmetries in the base-isolated structure considered here are due to the variation in: (i) the stiffness provided by the columns at the superstructure, labeled "superstructure eccentricity"; (ii) the stiffness of the isolation systems; and (iii) the yield strength or friction coefficient in the elastomeric or sliding isolation systems, respectively. The eccentricities arising at the base-raft due to dissimilar isolator properties are labeled as "isolation eccentricities". Only unidirectional eccentricities along the x-direction on the same side of the CM are considered for both superstructure and isolation eccentricities as suggested by Ryan and Chopra (2004). The two orthogonal components of earthquake ground acceleration are applied along the x- and y-directions considering the interaction effect between the responses, thereby closely modeling the actual behavior of the base-isolated structure during events of impact.

Different approaches to the modeling of the impact phenomena were adopted in previous studies (Anagnostopoulos, 1988, 2004; Anagnostopoulos and Spiliopoulos, 1992; Davis, 1992; Dimova, 2000). However, the adjacent structures, such as retaining walls, entry bridges etc. surrounding the base-isolated structure on all four sides, are characterized using the stiffness and damping properties in the present study. Such modeling has been effectively used for the vibro-impact problems in the case of base-isolated buildings in previous studies (Maison and Ventura, 1992; Malhotra, 1997; Nagarajaiah and Sun, 2001; Matsagar and Jangid, 2003). Note that the analysis is thus performed without using any gap elements or assuming values of the coefficient of restitution and the duration of impact. The adjacent structures are

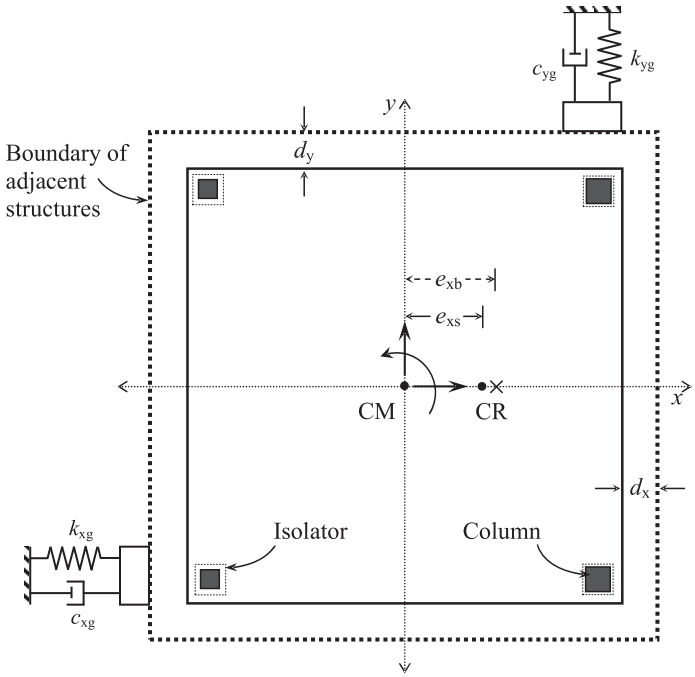

Figure 2. Location of adjacent structures and eccentricities in the torsionally coupled isolated structure.

considered to be situated at separation gap distances, d_x and d_y from the base-raft of the isolated structure, respectively in the x- and y-directions (Figure 2). The following assumptions are made for the structural system under consideration:

1. The point of impact is assumed to be exactly at the location of the base-raft, which is rigid in its own plane owing to diaphragm action.
2. The impact with adjacent structures is considered on all sides of the base-isolated structure, however the adjacent structures in any one direction are considered to be equal distances on either side.
3. The superstructure is considered to remain within the elastic limit during the earthquake excitation and impact phenomena.
4. The effects of soil–structure interaction are not taken into consideration.

3. GOVERNING EQUATIONS OF MOTION

For the system under consideration, the governing equations of motion are obtained by considering the equilibrium of forces in the direction of each degree-of-freedom. Two types of eccentricities are considered, namely superstructure eccentricity and isolation eccentricity respectively at the top-deck and the base-raft, as follows.

3.1. Asymmetries of the Superstructure

The governing equations of motion for the superstructure (top-deck) of the base-isolated system under earthquake ground excitation can be written as

$$\begin{bmatrix} m_s & 0 & 0 \\ 0 & m_s & 0 \\ 0 & 0 & m_s r_s^2 \end{bmatrix} \begin{Bmatrix} \ddot{u}_{xs} \\ \ddot{u}_{ys} \\ \ddot{u}_{\theta s} \end{Bmatrix} + [C] \begin{Bmatrix} \dot{u}_{xs} \\ \dot{u}_{ys} \\ \dot{u}_{\theta s} \end{Bmatrix}$$
$$+ \begin{bmatrix} K_{xs} & 0 & -K_{xs}e_{ys} \\ 0 & K_{ys} & K_{ys}e_{xs} \\ -K_{xs}e_{ys} & K_{ys}e_{xs} & K_{\theta s} \end{bmatrix} \begin{Bmatrix} u_{xs} \\ u_{ys} \\ u_{\theta s} \end{Bmatrix}$$
$$= - \begin{bmatrix} m_s & 0 & 0 \\ 0 & m_s & 0 \\ 0 & 0 & m_s r_s^2 \end{bmatrix} \begin{Bmatrix} \ddot{u}_{xb} + \ddot{u}_{xg} \\ \ddot{u}_{yb} + \ddot{u}_{yg} \\ \ddot{u}_{\theta b} \end{Bmatrix} \tag{1}$$

where m_s and r_s are the mass and radius of gyration of the top-deck about the vertical axis passing through the CM of the top-deck; $K_{xs} = \sum_i k_{xi}$ and $K_{ys} = \sum_i k_{yi}$ are the stiffness of the superstructure in the x- and y-directions, respectively (k_{xi} and k_{yi} represent the lateral stiffness of ith column); $K_{\theta s} = \sum_i \left(k_{xi} y_i^2 + k_{yi} x_i^2\right)$ is the torsional stiffness; $[C]$ is the damping matrix; u_{xs} and u_{ys} are the lateral displacements of the top-deck in the x- and y-directions, respectively; $u_{\theta s} = r_s \theta_s$ is the torsional displacement expressed in terms of the rotation, θ_s of the top-deck; and $\ddot{u}_{xg}$ and $\ddot{u}_{yg}$ are the ground acceleration in the x- and y-directions, respectively. The lateral displacements of the base-raft in the x- and y-directions are u_{xb} and u_{yb}, respectively; and $u_{\theta b} = r_b \theta_b$ is the torsional displacement expressed in terms of the rotation θ_b of the base-raft. Here, x_i and y_i represent the distance of ith column from the CM of the top-deck respectively in the x- and y-directions, and the over-dots denote differentiation with respect to time. The torsional stiffnesses of each individual column cross-section are negligible and therefore ignored. The uncoupled frequency parameters of the system are defined as follows:

$$\omega_{xs} = \sqrt{\frac{K_{xs}}{m_s}}, \quad \omega_{ys} = \sqrt{\frac{K_{ys}}{m_s}} \quad \text{and} \quad \omega_{\theta s} = \sqrt{\frac{K_{\theta s}}{m_s r_s^2}}. \tag{2}$$

The frequencies ω_{xs}, ω_{ys} and $\omega_{\theta s}$ are the natural frequencies of the superstructure if it were torsionally uncoupled, i.e. a system with $e_{xs} = 0$, with m_s, K_{xs}, K_{ys} and $K_{\theta s}$ the same as in the torsionally coupled system. Here, the eccentricity in the x-direction between the CM of the top-deck and the CR of the columns is given by

$$e_{xs} = \frac{1}{K_{ys}} \sum_i k_{yi} x_i. \tag{3}$$

3.2. Asymmetries of the Isolation System

Similarly, the governing equations of motion can be obtained for the base-raft as follows:

$$\begin{bmatrix} m_b & 0 & 0 \\ 0 & m_b & 0 \\ 0 & 0 & m_b r_b^2 \end{bmatrix} \begin{Bmatrix} \ddot{u}_{xb} \\ \ddot{u}_{yb} \\ \ddot{u}_{\theta b} \end{Bmatrix} + \begin{Bmatrix} F_{xb} \\ F_{yb} \\ F_{\theta b} \end{Bmatrix} - [C] \begin{Bmatrix} \dot{u}_{xs} \\ \dot{u}_{ys} \\ \dot{u}_{\theta s} \end{Bmatrix}$$
$$- \begin{bmatrix} K_{xs} & 0 & -K_{xs}e_{ys} \\ 0 & K_{ys} & K_{ys}e_{xs} \\ -K_{xs}e_{ys} & K_{ys}e_{xs} & K_{\theta s} \end{bmatrix} \begin{Bmatrix} u_{xs} \\ u_{ys} \\ u_{\theta s} \end{Bmatrix}$$
$$= - \begin{bmatrix} m_b & 0 & 0 \\ 0 & m_b & 0 \\ 0 & 0 & m_b r_b^2 \end{bmatrix} \begin{Bmatrix} \ddot{u}_{xg} \\ \ddot{u}_{yg} \\ 0 \end{Bmatrix} \tag{4}$$

where m_b and r_b are the mass and radius of gyration of the base-raft about the vertical axis through the CM of the base-raft, respectively; $F_{xb} = \sum_j f_{xbj}$ and $F_{yb} = \sum_j f_{ybj}$ (f_{xbj} and f_{ybj} represent the isolation forces in the jth bearing developed in the x- and y-directions, respectively); $F_{\theta b} = \sum_i \left(f_{xbj} y_j^2 + f_{ybj} x_j^2 \right)$ is the torsional force. Here, x_j and y_j represent the distance of the jth isolator from the CM of the base-raft respectively in the x- and y-directions. The torsional stiffness of each individual isolation system is negligible and hence ignored. The uncoupled frequency parameters of the system are defined as follows:

$$\omega_{xb} = \sqrt{\frac{K_{xb}}{(m_s + m_b)}}, \quad \omega_{yb} = \sqrt{\frac{K_{yb}}{(m_s + m_b)}} \quad \text{and} \quad \omega_{\theta b} = \sqrt{\frac{K_{\theta b}}{(m_s + m_b)\, r_b^2}} \tag{5}$$

where $K_{xb} = \sum_j k_{xbj}$ and $K_{yb} = \sum_j k_{ybj}$ are the isolation stiffnesses in the x- and y-directions, respectively (k_{xbj} and k_{ybj} represent the bearing stiffnesses of the jth isolator); $K_{\theta b} = \sum_j \left(k_{xbj} y_j^2 + k_{ybj} x_j^2 \right)$ is the torsional stiffness. The frequencies ω_{xb}, ω_{yb} and $\omega_{\theta b}$ are the natural frequencies of the isolation system if it were torsionally uncoupled, i.e. a system with $e_{xb} = 0$, with m_s, m_b, K_{xb}, K_{yb} and $K_{\theta b}$ the same as in the coupled system. Here, the eccentricity between the CM of the base-raft and the CR of the bearings is given by

$$e_{xb} = \frac{1}{K_{yb}} \sum_j k_{ybj} x_j + e_{xf} \tag{6}$$

where the isolation eccentricity arising due to the differences in the yield strength may be separately denoted as

$$e_{xf} = \frac{1}{F_{yb}} \sum_j f_{ybj} x_j. \tag{7}$$

The impact between the base-isolated structure and the adjacent structure occurs in the following two conditions:

$$|u_{xb}| + \frac{B}{2} |u_{\theta b}| > d_x, \tag{8}$$

$$\left|u_{yb}\right| + \frac{B}{2} |u_{\theta b}| > d_y. \tag{9}$$

A system of differential equations of equilibrium for the base-raft during impact with the adjacent structures becomes

$$\begin{bmatrix} m_b & 0 & 0 \\ 0 & m_b & 0 \\ 0 & 0 & m_b r_b^2 \end{bmatrix} \begin{Bmatrix} \ddot{u}_{xb} \\ \ddot{u}_{yb} \\ \ddot{u}_{\theta b} \end{Bmatrix} + \begin{Bmatrix} F_{xb} \\ F_{yb} \\ F_{\theta b} \end{Bmatrix} + \begin{Bmatrix} f_{xi} \\ f_{yi} \\ f_{\theta i} \end{Bmatrix}$$
$$- [C] \begin{Bmatrix} \dot{u}_{xs} \\ \dot{u}_{ys} \\ \dot{u}_{\theta s} \end{Bmatrix} - \begin{bmatrix} K_{xs} & 0 & -K_{xs} e_{ys} \\ 0 & K_{ys} & K_{ys} e_{xs} \\ -K_{xs} e_{ys} & K_{ys} e_{xs} & K_{\theta s} \end{bmatrix} \begin{Bmatrix} u_{xs} \\ u_{ys} \\ u_{\theta s} \end{Bmatrix}$$
$$= - \begin{bmatrix} m_b & 0 & 0 \\ 0 & m_b & 0 \\ 0 & 0 & m_b r_b^2 \end{bmatrix} \begin{Bmatrix} \ddot{u}_{xg} \\ \ddot{u}_{yg} \\ 0 \end{Bmatrix}. \tag{10}$$

In equation 10 the impact forces are defined as

$$f_{xi} = k_{xg}(|u_{xb}| - d_x) \operatorname{sgn}(u_{xb}) + c_{xg} \dot{u}_{xb}, \tag{11}$$

$$f_{yi} = k_{yg}(\left|u_{yb}\right| - d_y) \operatorname{sgn}(u_{yb}) + c_{yg} \dot{u}_{yb}, \tag{12}$$

$$f_{\theta i} = [k_{xg}(|u_{xb}| - d_x) + c_{xg} \dot{u}_{xb}] u_{yb} + [k_{yg}(\left|u_{yb}\right| - d_y) + c_{yg} \dot{u}_{yb}] u_{xb}, \tag{13}$$

where k_{xg} and k_{yg} are the stiffnesses of the adjacent structures in the x- and y-directions, respectively; c_{xg} and c_{yg} are the damping coefficients of the adjacent structures in the x- and y-directions, respectively; and sgn denotes the signum function.

The restoring forces developed in the bearings depend upon the type of isolation systems utilized. The choice of isolation systems and analysis procedure has to be made so as to predict properly the seismic response leading to a rational and economical design. The guide specifications for seismic design of structures (BSSC, 1997; UBC, 1997; AASHTO, 1999) suggest the use of the time-history nonlinear dynamic analysis of base-isolated structures. It is also recommended that a linear equivalent mathematical model can be adopted to

carry out an equivalent static analysis to design the bearings and the superstructure. Three commonly used isolation systems are considered in the present study, the force-deformation characteristics of which are described below.

3.3. High-damping Rubber Bearing

The popularly used high-damping rubber bearings (HDRB) comprise steel and rubber plates built through a vulcanization process in the alternate layers. The dominant feature of HDRB is parallel action of the linear spring and damping. The HDRB are characterized by high damping capacity, horizontal flexibility and high vertical stiffness (Tsopelas et al., 1991; Kikuchi and Aiken, 1997; Koo et al., 1999). Here, the code-specified equivalent linear viscous model is adopted. A schematic diagram of the HDRB is shown in Figure 3a, which represents the linear stiffness with viscous damping for bi-directional excitation. It is to be noted that such an equivalent linear model of an isolation system is quite simple and generally accurately predicts the results except for a few typical isolator parameters (Matsagar and Jangid, 2004). The restoring force developed in the HDRB is given by

$$\begin{Bmatrix} f_{xbj} \\ f_{ybj} \end{Bmatrix} = \begin{bmatrix} c_{xbj} & 0 \\ 0 & c_{ybj} \end{bmatrix} \begin{Bmatrix} \dot{u}_{xbj} \\ \dot{u}_{ybj} \end{Bmatrix} + \begin{bmatrix} k_{xbj} & 0 \\ 0 & k_{ybj} \end{bmatrix} \begin{Bmatrix} u_{xbj} \\ u_{ybj} \end{Bmatrix} \tag{14}$$

where $c_{xbj} = c_{ybj}$ and $k_{xbj} = k_{ybj}$ are the damping and stiffness of HDRB, respectively in the x- and y-directions for the jth isolator, owing to the isotropic nature of individual isolation systems. Therefore, note that the isolation time periods T_b in the x- and y-directions are the same.

The linear stiffness and equivalent viscous damping of the HDRB is selected to provide the specific values of the two parameters, namely, the isolation time period (T_b) and the effective damping ratio (β_{eff}) defined as

$$T_b = 2\pi \sqrt{\frac{(m_s + m_b)}{K_{xb}}}, \tag{15}$$

$$\beta_{eff} = \frac{\sum_j c_{xbj}}{2(m_s + m_b)\omega_{xb}}, \tag{16}$$

where $\omega_{xb} = 2\pi/T_b$ is the isolation frequency.

3.4. Lead-rubber Bearing

These bearings are similar to the HDRB except that a central lead core is used to provide additional means of energy dissipation and initial rigidity against minor earthquakes and winds (Skinner et al., 1975; Robinson, 1982). In lead-rubber bearings (LRB), the energy absorbing capacity by the lead core reduces the isolation level displacement. The LRB also provide an additional hysteretic damping through the yielding of the lead core. The force–deformation behavior of the LRB is generally represented by nonlinear hysteretic characteristics. For the

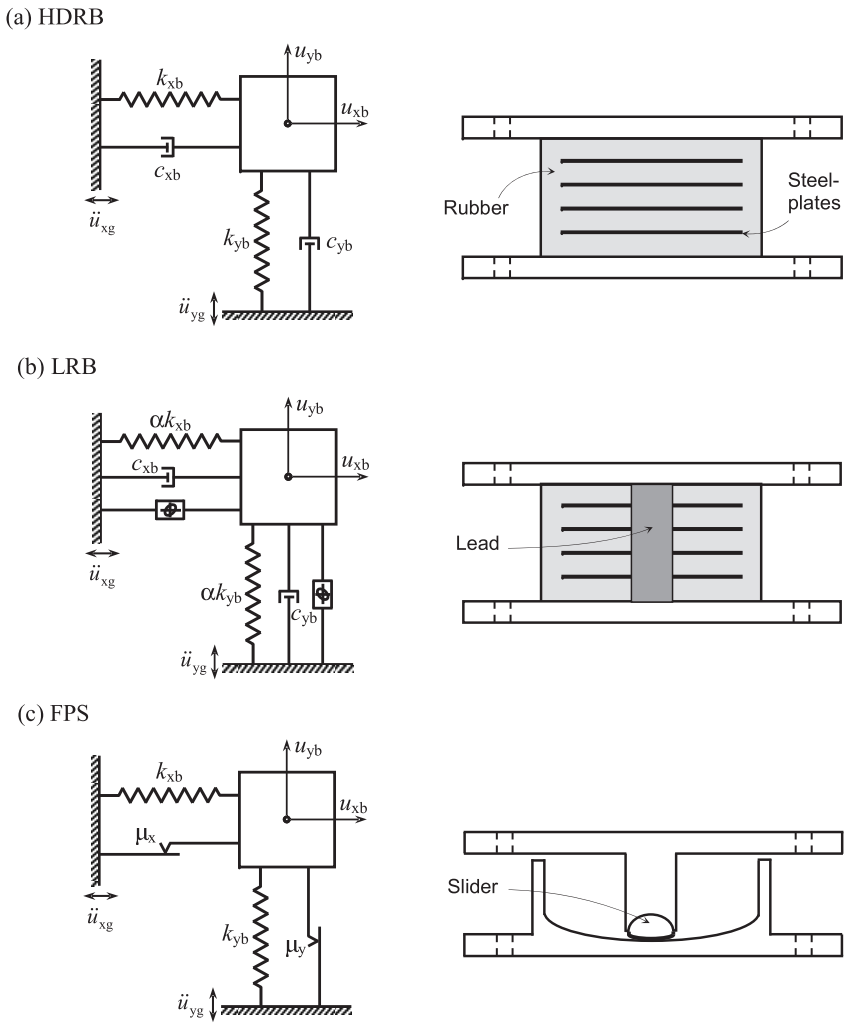

Figure 3. Schematic diagrams for HDRB, LRB and the FPS.

present study, a nonlinear model (Park et al., 1986) is used to characterize the hysteretic behavior of the LRB, the schematic diagram of which is shown in Figure 3b for bi-directional excitation. The restoring force developed in the LRB is given by

$$\begin{Bmatrix} f_{xbj} \\ f_{ybj} \end{Bmatrix} = \begin{bmatrix} c_{xbj} & 0 \\ 0 & c_{ybj} \end{bmatrix} \begin{Bmatrix} \dot{u}_{xbj} \\ \dot{u}_{ybj} \end{Bmatrix} + \alpha \begin{bmatrix} k_{xj} & 0 \\ 0 & k_{yj} \end{bmatrix} \begin{Bmatrix} u_{xbj} \\ u_{ybj} \end{Bmatrix} + (1-\alpha) \begin{Bmatrix} f_{xj}^{y} \\ f_{yj}^{y} \end{Bmatrix} \begin{Bmatrix} Z_{xj} \\ Z_{yj} \end{Bmatrix} \tag{17}$$

where $f_{xj}^y = f_{yj}^y$ are the yield strengths of the jth bearing in the x- and y-directions; α is an index which represents the ratio of post- to pre-yielding stiffness; $k_{xj} = k_{yj}$ are the pre-yield stiffnesses; and $Z_{xj} = Z_{yj}$ are the nondimensional hysteretic displacement components satisfying the following nonlinear first-order differential equation:

$$q_j \begin{Bmatrix} \frac{dZ_{xj}}{dt} \\ \frac{dZ_{yj}}{dt} \end{Bmatrix} = \begin{bmatrix} A - \beta \left|\dot{u}_{xbj}\right| Z_{xj} \left|Z_{xj}\right|^{n-1} - \tau Z_{xj}^n & -\beta \left|\dot{u}_{ybj}\right| Z_{yj} \left|Z_{xj}\right|^{n-1} - \tau Z_{xj} Z_{yj}^n \\ -\beta \left|\dot{u}_{xbj}\right| Z_{xj} \left|Z_{yj}\right|^{n-1} - \tau Z_{yj} Z_{xj}^n & A - \beta \left|\dot{u}_{ybj}\right| Z_{yj} \left|Z_{yj}\right|^{n-1} - \tau Z_{yj}^n \end{bmatrix} \times \begin{Bmatrix} \dot{u}_{xbj} \\ \dot{u}_{ybj} \end{Bmatrix} \tag{18}$$

where q_j is the yield displacement of the jth isolator; dimensionless parameters β, τ, A and n are selected such that the predicted response from the model closely matches the experimental results. The parameter n is an integer constant, which controls the smoothness of the transition from an elastic to an inelastic response.

The LRB are characterized by the isolation time period (T_b), the damping ratio (ξ_b) and the normalized yield strengths ($f_{xj}^y/W = f_{yj}^y/W$). Here, $W = (m_s + m_b)g$ is the total weight of the structure; and g is the acceleration due to gravity. The isolation parameter T_b is computed from equation 15 using the post-yield stiffness k_{xbj} of the isolator and the damping is $\xi_b = \sum_j c_{xbj}/2(m_s + m_b)\omega_{xb}$. The other parameters of the LRB are held constant with q_j = 2.5 cm, $\beta = \tau = 0.5$, $A = 1$ and $n = 2$.

3.5. Friction Pendulum System

The concept of sliding systems used along with the notion of a pendulum type response, by means of an articulated slider on the spherical concave chrome surface, marks a friction pendulum system (FPS) (Zayas et al., 1990). The isolation system is activated only when the earthquake forces overcome the static value of friction. The FPS develops a lateral force equal to the combination of the mobilized frictional force and the restoring force that develops because of the rising of the structure along the spherical concave surface. The schematic diagram of the FPS is shown in Figure 3c for bi-directional excitation. The resisting force provided by the system is

$$\begin{Bmatrix} f_{xbj} \\ f_{ybj} \end{Bmatrix} = \begin{bmatrix} k_{xbj} & 0 \\ 0 & k_{ybj} \end{bmatrix} \begin{Bmatrix} u_{xbj} \\ u_{ybj} \end{Bmatrix} + \begin{Bmatrix} f_{xj} \\ f_{yj} \end{Bmatrix} \tag{19}$$

where $k_{xbj} = k_{ybj}$ are the bearing stiffnesses provided by virtue of inward gravity action at the concave surface; and $f_{xj} = f_{yj}$ are the limiting frictional forces, respectively in the x- and y-directions.

The system is characterized by the isolation time period (T_b) that depends upon the radius of curvature of the concave surface and the friction coefficient ($\mu = \mu_{xj} = \mu_{yj}$). The isolation stiffnesses $k_{xbj} = k_{ybj}$ are adjusted so that the specified value of the isolation time period evaluated by equation 15 is achieved.

Table 1. Properties of the earthquake ground motions selected.

Earthquake	Component	Event	Recording station	PGA (g)
Loma Prieta, 1989	N00E	October 18th, 1989	Los Gatos	0.559
	N90E		Presentation Center	0.596
Northridge, 1994	N90S	January 17th, 1994	Sylmar Converter Center	0.593
	N360S			0.827
Kobe, 1995	EW	January 17th, 1995	JMA (Japan	0.617
	NS		Meteorological Agency)	0.818

4. SOLUTION OF EQUATIONS OF MOTION

A classical modal superposition technique cannot be employed in the solution of equations of motion as (i) the system is nonclassically damped because of a difference in the damping in isolation systems compared to the damping in the superstructure, and (ii) the force– deformation behavior of LRB and sliding systems is nonlinear. Therefore, the equations of motion are solved numerically using Newmark's method of step-by-step integration, adopting linear variation of acceleration over a small time interval of Δt. The time interval for solving the equations of motion is taken as 0.02/20 s (i.e. $\Delta t = 0.001$ s).

5. NUMERICAL STUDY

The seismic response of a single-story asymmetric base-isolated structure is investigated under various real earthquake ground motions during impact with the adjacent structures. The parametric studies are carried out using a mathematical model of the torsionally coupled base-isolated structure under consideration for calculation of the response quantities of interest such as the peak top-deck absolute acceleration and the peak relative base-raft displacement. The above response quantities are important because the floor accelerations developed in the superstructure are proportional to the forces exerted due to earthquake ground motion and the base-raft displacements are crucial in the design of isolation systems. The earthquake ground motions used in the present study and associated peak ground acceleration (PGA) are summarized in Table 1.

For the present study, the mass of the top-deck, i.e. m_s, and the stiffnesses $K_{xs} = K_{ys}$ of the columns supporting it are selected to provide the required fundamental time period of the superstructure as a fixed base, T_s. The damping matrix of the superstructure $[C_s]$ is not known explicitly. The modal damping ratio is kept constant in all modes of vibration. Thus, the model of the isolated structural system under consideration can be completely characterized by specifying the parameters, namely, the fundamental time period of the superstructure (T_s), the damping ratio of the superstructure (ξ_s) which is kept constant for all modes, the mass ratio m_b/m_s, the torsional coupling parameters and the isolation system properties. For the numerical study, the superstructure damping $\xi_s = 0.05$ and the mass ratio $m_b/m_s = 1$ are held constant. The torsional coupling parameters considered for the superstructure eccentricity can be summarized as

$$\Omega_s = \frac{\omega_{\theta s}}{\omega_{xs}} = \frac{\omega_{\theta s}}{\omega_{ys}} \tag{20}$$

and that for the isolation eccentricity as

$$\Omega_b = \frac{\omega_{\theta b}}{\omega_{xb}} = \frac{\omega_{\theta b}}{\omega_{yb}}. \tag{21}$$

The two other system parameters are eccentricities that are expressed as eccentricity ratios, normalized with the plan dimension B as e_{xs}/B and e_{xb}/B for a square configuration of the top-deck and base-raft, i.e. $B = D$.

The adjacent structures are considered on all four sides with appropriate separation (isolation/moat) gap distances d_x and d_y in the x- and y-directions, respectively, characterized by the stiffnesses k_{xg}, k_{yg} and damping coefficients c_{xg}, c_{yg}. The stiffnesses k_{xg} and k_{yg} are selected as some fraction of superstructure stiffness of the isolated structure, expressed as the stiffness ratio, $k_{xr} = k_{xg}/K_{xs}$, $k_{yr} = k_{yg}/K_{ys}$, and the damping ratio for the adjacent structures, ξ_{xg} and ξ_{yg}, are chosen to be the same as that in the superstructure of the isolated structure; thus, adjacent structures are modeled realistically. The comparative performance of the structure isolated by various commonly used isolation systems such as HDRB, LRB and the FPS is investigated for the impact response under seismic excitation. Further, the effects of impact on torsionally coupled base-isolated structures are compared with those of torsionally uncoupled base-isolated structures.

5.1. Effect of Torsional Impact on Response

Figure 4 illustrates the time variation of the top-deck absolute acceleration and relative base-raft displacement of a single-story structure isolated by the HDRB with and without impact conditions under the Loma Prieta, 1989, earthquake applied along two directions simultaneously. The parameters of the HDRB considered are $T_b = 2$ s and $\beta_{eff} = 0.1$ with the adjacent structures at separation gap distances $d_x = d_y = 4$ cm and stiffness ratios $k_{xr} = k_{yr} = 5 \times 10^{-4}$. Note that the gap distances selected in this study and the stiffness of adjacent structures resembles closely most of the similar site conditions prevailing at base-isolated buildings in the California region. The torsional coupling parameters are chosen as eccentricities, $e_{xs}/B = e_{xb}/B = e_{xf}/B = 0.3$, and frequency ratios, $\Omega_s = \Omega_b = 1$, representing a torsionally tuned system with moderate eccentricity at the superstructure and isolation levels both on the same side of the CM. The plot indicates that, due to the impact of a torsionally coupled isolated structure upon adjacent structures, the acceleration in the top-deck increased compared to that without any impact. On the other hand, the top-deck acceleration of the torsionally uncoupled structure is higher than that of the coupled counterpart during no impact conditions. The number of cycles of acceleration increases when impact occurs, which is a commonly observed phenomenon in torsionally coupled and uncoupled cases. This implies that by ignoring the torsional coupling in lateral and torsional displacements the top-deck acceleration would be over-predicted. Due to the occurrence of impact, there is a substantial increase in the top-deck acceleration. Although the benefits of base isolation are diminished due to occurrence of impact, the isolation is still effective in reducing the earthquake response of the structures when compared to the top-deck acceleration

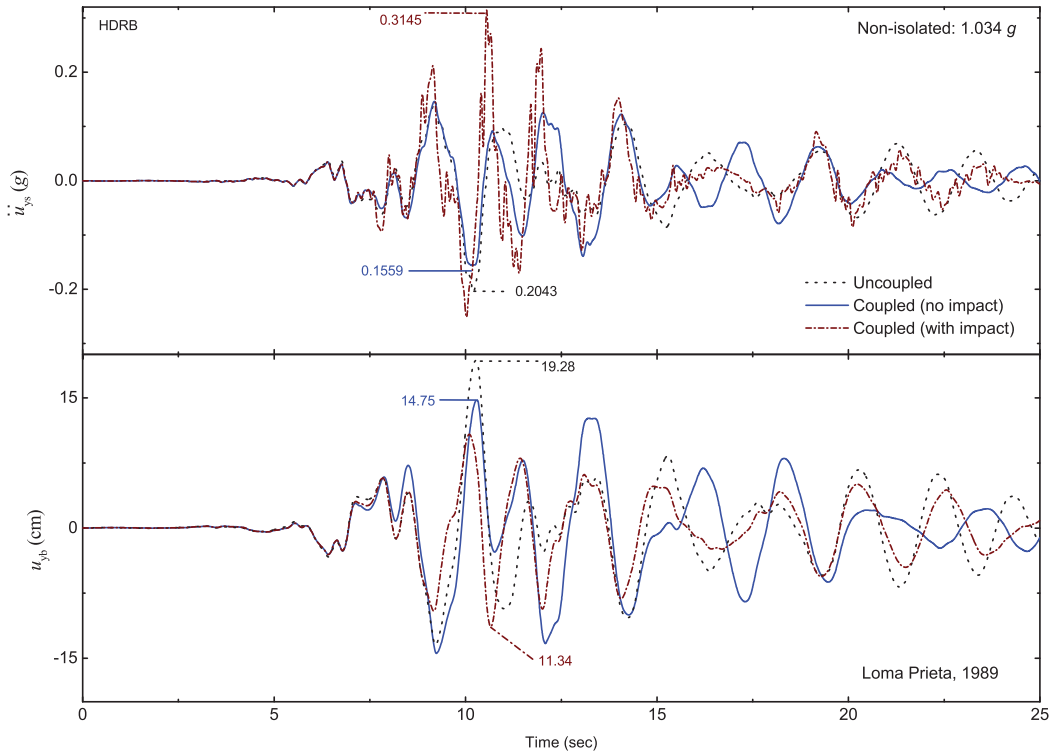

Figure 4. Time history for top-deck acceleration and base-raft displacement for torsionally uncoupled and coupled base-isolated structures using HDRB under the Loma Prieta, 1989, earthquake ($T_s = 0.25$ s, $T_b = 2$ s and $\beta_{eff} = 0.1$), $d_x = d_y = 4$ cm and $k_{xr} = k_{yr} = 5 \times 10^{-4}$.

in a nonisolated structure. Due to the increased superstructure accelerations imparted during impact, the capacity demand of the superstructure increases. The peak value of the coupled lateral displacement of the base-raft u_{yb} is 14.75 cm without impact and this reduced to 11.34 cm with impact, implying a decrease in base-raft displacement during impact conditions. In addition, it can be seen that the top-deck acceleration and base-raft displacement are overpredicted when torsional coupling is ignored. A similar trend of an increase in the top-deck acceleration and a reduction in the lateral displacement of the base-raft is observed during impact conditions when LRB ($T_b = 2.5$ s, $\xi_b = 0.05$, $q_j = 2.5$ cm and $f_{xj}^y / W = f_{yj}^y / W = 0.05$) and the FPS ($T_b = 2.5$ s and $\mu = 0.05$) are utilized, as shown in Figures 5 and 6, respectively, under the Loma Prieta, 1989, earthquake, maintaining all other parameters similar.

The peak top-deck absolute accelerations and lateral base-raft displacements computed for a single-story asymmetric isolated structure under two components of the Loma Prieta 1989, Sylmar 1994, and Kobe 1995 earthquake ground motions are compared in Table 2. The responses are obtained for torsionally coupled and uncoupled structures isolated using different systems such as HDRB, LRB and the FPS utilized for isolation with similar properties as used before. The quantities in parentheses pertain to the torsionally uncoupled conditions. The response of all the systems is shown in the cases of impact and no impact with isola-

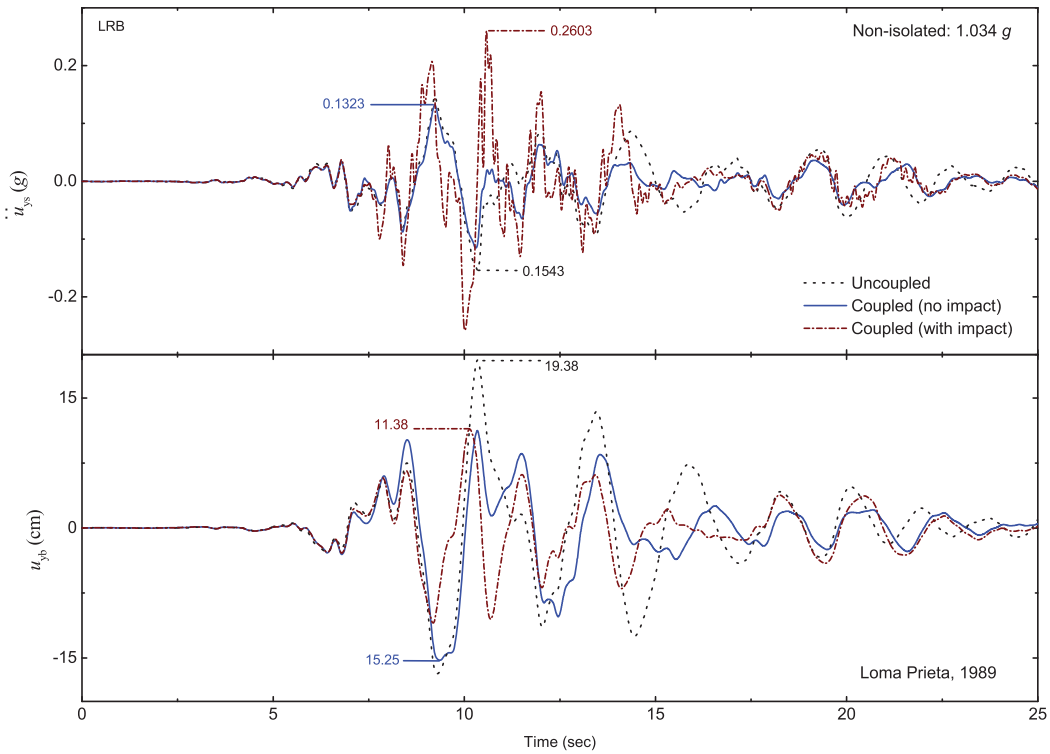

Figure 5. Time history for top-deck acceleration and base-raft displacement for torsionally uncoupled and coupled base-isolated structures using LRB under the Loma Prieta, 1989, earthquake ($T_s = 0.25$ s, $T_b = 2.5$ s, $\xi_b = 0.05$, $q_j = 2.5$ cm and $f_{xj}^y/W = f_{yj}^y/W = 0.05$), $d_x = d_y = 4$ cm and $k_{xr} = k_{yr} = 5 \times 10^{-4}$.

Table 2. Peak response of single-story asymmetric isolated structure with and without impact. Quantities in parentheses pertain to the torsionally uncoupled structure.

Quantity	Loma Prieta 1989				Northridge 1994				Kobe 1995			
Isolation systems	u_{xb} (cm)	u_{yb} (cm)	$\ddot{u}_{xs}$ (g)	$\ddot{u}_{ys}$ (g)	u_{xb} (cm)	u_{yb} (cm)	$\ddot{u}_{xs}$ (g)	$\ddot{u}_{ys}$ (g)	u_{xb} (cm)	u_{yb} (cm)	$\ddot{u}_{xs}$ (g)	$\ddot{u}_{ys}$ (g)
HDRB												
No impact	53.61 (53.61)	14.75 (19.28)	0.547 (0.547)	0.156 (0.204)	34.26 (34.26)	41.28 (49.42)	0.352 (0.352)	0.451 (0.498)	16.59 (16.59)	23.68 (32.30)	0.177 (0.177)	0.320 (0.345)
With impact	21.79 (21.95)	11.34 (13.50)	0.709 (0.727)	0.315 (0.426)	18.09 (17.61)	27.37 (29.20)	0.489 (0.500)	0.726 (0.836)	14.21 (14.53)	17.19 (22.28)	0.481 (0.531)	0.501 (0.752)
LRB												
No impact	52.43 (52.50)	15.25 (19.38)	0.365 (0.365)	0.132 (0.154)	44.89 (46.68)	46.33 (55.14)	0.300 (0.314)	0.325 (0.388)	16.96 (17.16)	23.47 (28.20)	0.124 (0.136)	0.171 (0.213)
With impact	24.66 (24.69)	11.38 (12.68)	0.610 (0.645)	0.260 (0.394)	19.16 (18.55)	29.07 (30.90)	0.477 (0.485)	0.700 (0.756)	13.13 (13.44)	17.24 (20.19)	0.426 (0.446)	0.446 (0.635)
FPS												
No impact	52.84 (52.96)	17.41 (21.18)	0.367 (0.366)	0.153 (0.180)	49.41 (52.29)	47.66 (65.41)	0.324 (0.351)	0.318 (0.470)	17.12 (17.14)	23.45 (25.83)	0.151 (0.144)	0.165 (0.219)
With impact	25.60 (25.57)	11.41 (11.94)	0.618 (0.665)	0.264 (0.344)	18.95 (18.56)	29.43 (31.09)	0.484 (0.454)	0.698 (0.774)	12.94 (13.27)	17.59 (20.09)	0.403 (0.402)	0.446 (0.617)
Non-isolated	–		1.230	1.034	–		0.840	1.653	–		0.902	1.500

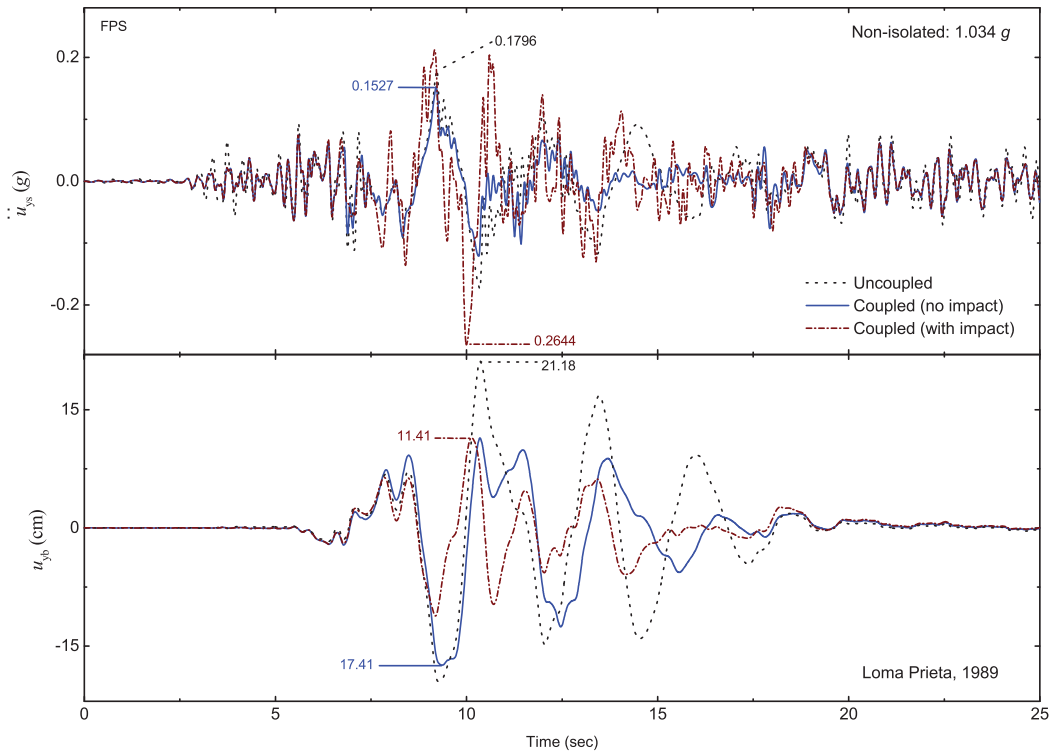

Figure 6. Time history for top-deck acceleration and base-raft displacement for torsionally uncoupled and coupled base-isolated structures using the FPS under the Loma Prieta, 1989, earthquake ($T_s = 0.25$ s, $T_b = 2.5$ s and $\mu = 0.05$), $d_x = d_y = 4$ cm and $k_{xr} = k_{yr} = 5 \times 10^{-4}$.

tion gap distances $d_x = d_y = 4$ cm and stiffness ratios $k_{xr} = k_{yr} = 5 \times 10^{-4}$. It is seen that during impact also a similar trend of prediction of increased acceleration in the uncoupled structure over that in the coupled structure is observed. These results also indicate that the top-deck acceleration increases due to the impact between the isolated structure and the adjacent structures. On the other hand, reduction in the lateral displacement of the base-raft is also observed pertaining to the impact event.

Figure 7 shows a comparison of the FFT (Fast Fourier Transform) amplitude spectra of the corresponding top-deck acceleration for single-story torsionally coupled and uncoupled structures isolated by HDRB, LRB and the FPS under the Loma Prieta, 1989, earthquake ground motion with and without impact (refer to Figures 4 to 6 for the time history of the top-deck acceleration). It is seen that the FFT amplitudes are reduced when torsional coupling is considered. These results also show that due to impact of isolated structures upon adjacent structures the FFT amplitudes of the top-deck acceleration are increased which confirms the reduction in effectiveness of the isolation pertaining to impact. Notably, there is significant increase in the FFT amplitudes associated with high-frequency content. The increase in acceleration associated with high-frequency content can be detrimental to the high-frequency sensitive equipment installed in the structure, if impact takes place. Further, the top-deck ac-

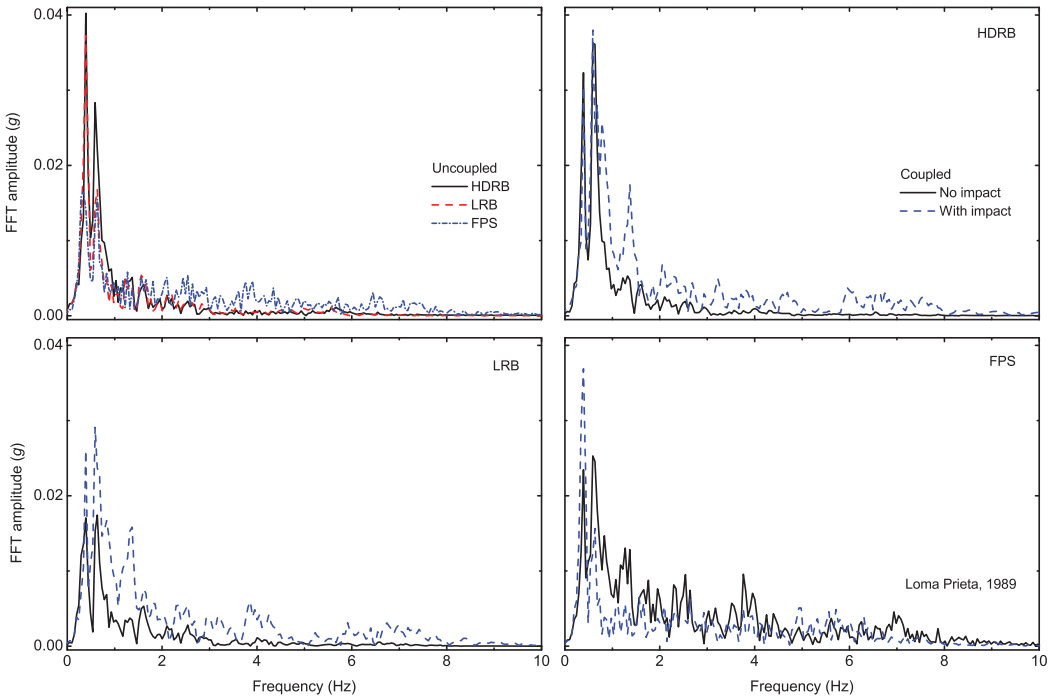

Figure 7. Frequency plots of top-deck acceleration for nonisolated ($T_s = 0.25$ s) and base-isolated structures using HDRB ($T_b = 2$ s and $\beta_{eff} = 0.1$), LRB ($T_b = 2.5$ s, $\xi_b = 0.05$, $q_j = 2.5$ cm and $f_{xj}^y/W = f_{yj}^y/W = 0.05$) and the FPS ($T_b = 2.5$ s and $\mu = 0.05$) under the Loma Prieta, 1989, earthquake with $d_x = d_y = 4$ cm and $k_{xr} = k_{yr} = 5 \times 10^{-4}$.

celeration for the FPS reflects the contribution from higher frequencies as compared to the HDRB and LRB even if there is no impact.

5.2. Effect of eccentricities

As it is observed that the torsional coupling present in the isolated structure affects the seismic response greatly in impact and no impact cases, the study of the effects of increasing asymmetry in the structure is essential. Figures 8, 9 and 10 show plots of the ratios of the top-deck acceleration and the base-raft displacement obtained with and without impact, expressed as follows:

$$\Gamma_1 = \frac{(\ddot{u}_{xs})_{\text{With impact}}}{(\ddot{u}_{xs})_{\text{No impact}}} \quad \text{and} \quad \Gamma_2 = \frac{(\ddot{u}_{ys})_{\text{With impact}}}{(\ddot{u}_{ys})_{\text{No impact}}}, \tag{22}$$

$$\Gamma_3 = \frac{(u_{xb})_{\text{With impact}}}{(u_{xb})_{\text{No impact}}} \quad \text{and} \quad \Gamma_4 = \frac{(u_{yb})_{\text{With impact}}}{(u_{yb})_{\text{No impact}}}. \tag{23}$$

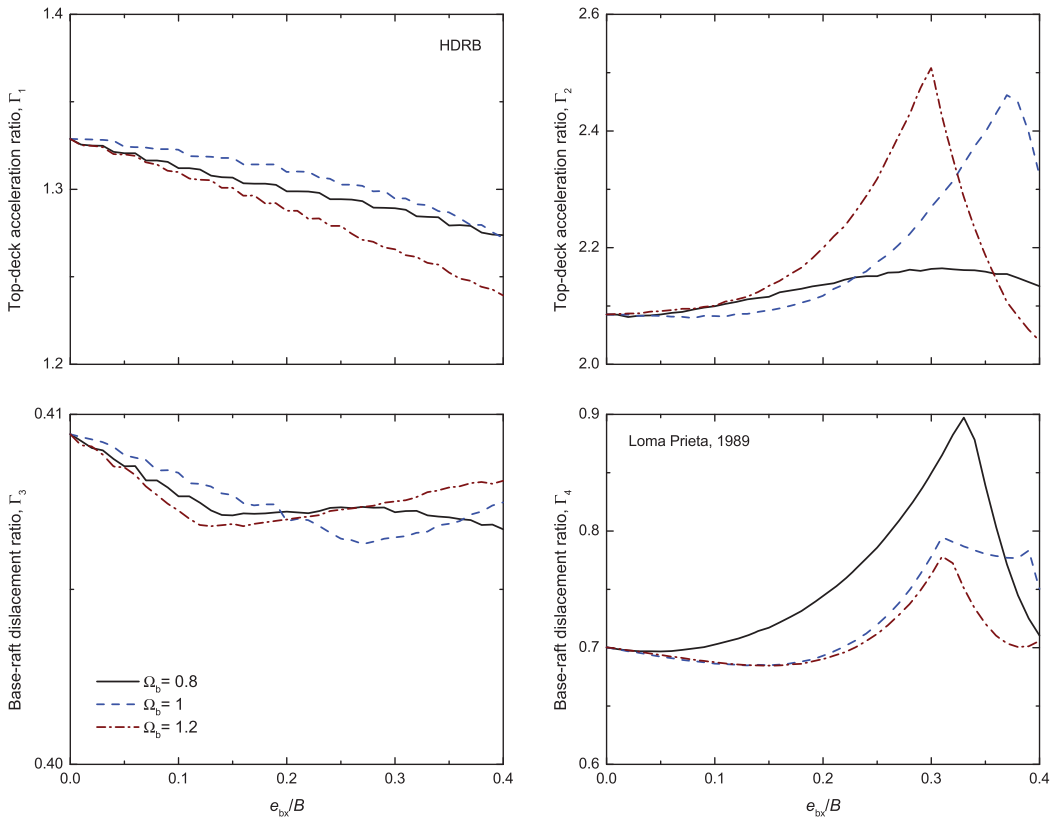

Figure 8. Effect of eccentricities on top-deck acceleration and base-raft displacement under the Loma Prieta, 1989, earthquake for HDRB ($T_b = 2$ s and $\beta_{eff} = 0.1$) with $k_{xr} = k_{yr} = 5 \times 10^{-4}$.

The results are obtained for the three isolation systems under consideration, namely, HDRB, LRB and the FPS during the action of different earthquakes and plotted against increasing eccentricity due to isolation stiffness, e_{bx}. The isolation gap distances $d_x = d_y = 4$ cm with constant stiffness ratios $k_{rx} = k_{ry} = 5 \times 10^{-4}$ were selected. The plots are obtained for frequency ratios $\Omega_b = 0.8$, 1 and 1.2 indicating torsionally flexible to stiff systems, and the isolation parameters the same as before. It can be observed that the increased torsional coupling has an adverse affect during impact of base-isolated structure upon adjacent structures, showing an increase in the seismic response.

5.3. Effect of separation gap distances and adjacent structure stiffnesses

In base-isolated structures, the separation (isolation/moat) gap distance is invariably provided to accommodate the displacements at isolation level. Owing to inappropriate provision of a separation gap distance or locking of the separation gap distance due to unexpected reasons, the chances of impact are increased; hence it is important to study the effect of separation gap distance on the impact response of base-isolated structures. Effects of variation in the

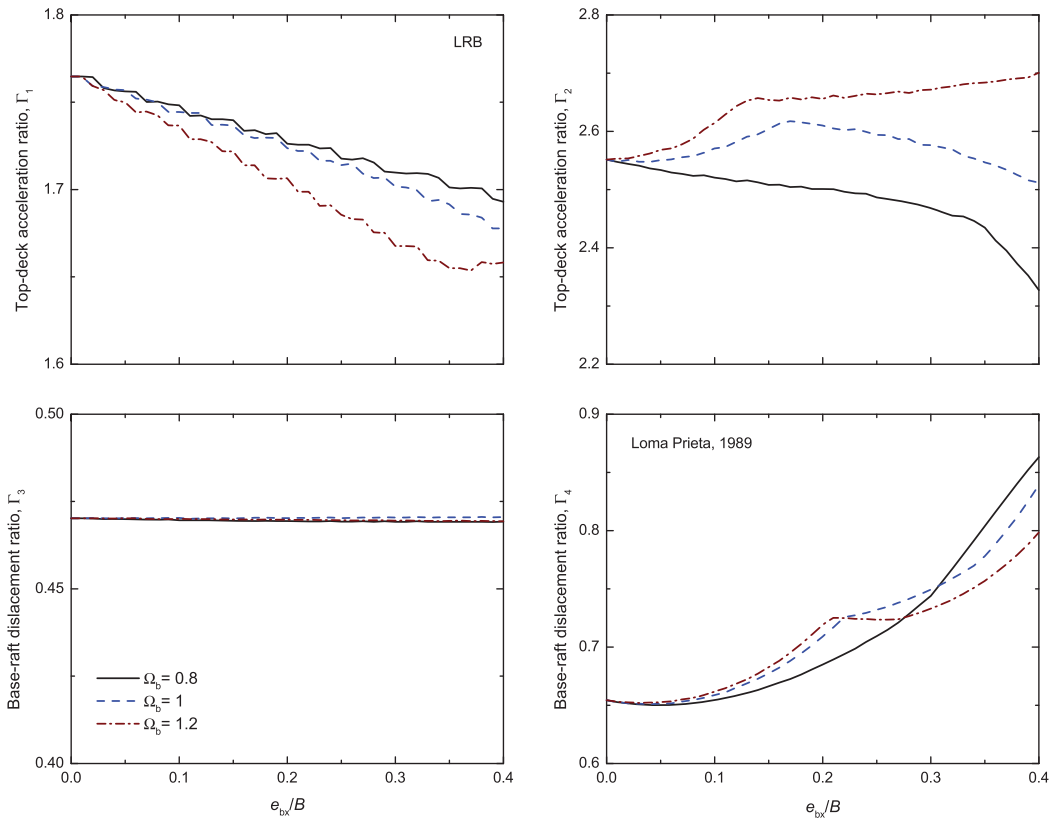

Figure 9. Effect of eccentricities on top-deck acceleration and base-raft displacement under the Loma Prieta, 1989, earthquake for LRB ($T_b = 2.5$ s, $\xi_b = 0.05$, $q_j = 2.5$ cm and $f_{xj}^y/W = f_{yj}^y/W = 0.05$) with $k_{xr} = k_{yr} = 5 \times 10^{-4}$.

separation gap distance on the superstructure acceleration and isolation level displacement are studied during different earthquakes for the torsionally coupled structures isolated by HDRB, LRB and the FPS as shown in Figures 11, 12 and 13, respectively. The responses are obtained by varying the gap distances (both d_x and d_y equally on either side) and they are plotted against normalized gap size under different earthquake ground motions. The normalization is carried out with the maximum gap distance beyond which there is no further occurrence of impact between the isolated and the adjacent structures. It can be observed that there is an initial increase in the top-deck acceleration up to a certain value of separation gap distance and then the acceleration decreases with further increase in the gap distances. The maximum increase in the top-deck acceleration for intermediate gap distances is because of the high velocity of the structure at the instant of impact.

Three values of the stiffness ratios $k_{xr} = k_{yr} = 5 \times 10^{-5}$, 5×10^{-4} and 10^{-3} are selected to study the effect of stiffness of the adjacent structures on the impact response of the base-isolated structure. It can be seen that with the increased stiffness ratio the top-deck acceleration increases because of increased impact forces. The impact response quantities

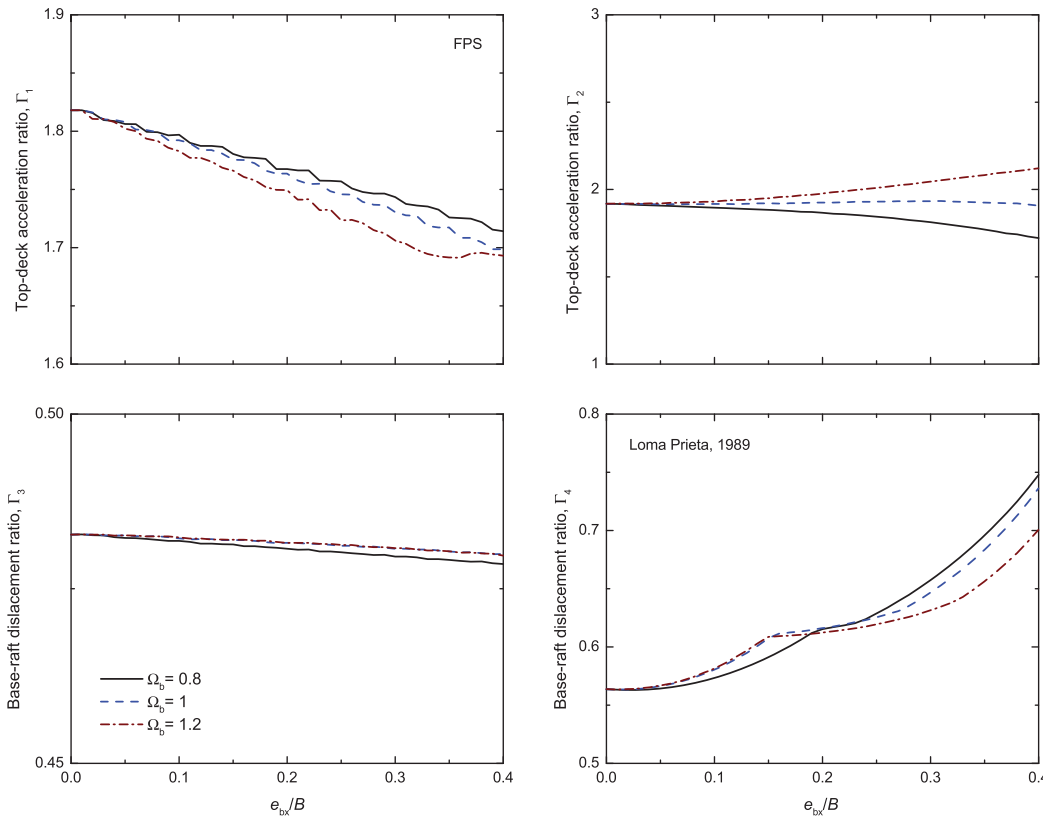

Figure 10. Effect of eccentricities on top-deck acceleration and base-raft displacement under the Loma Prieta, 1989, earthquake for FPS ($T_b = 2.5$ s and $\mu = 0.05$) with $k_{xr} = k_{yr} = 5 \times 10^{-4}$.

are found to be predominantly influenced by the stiffness of the adjacent structures. As expected, the base-raft displacement increases with increase of the isolation gap distance and decreases with increase in the stiffness of the adjacent structures.

5.4. Effect of Superstructure Flexibility

In order to study the effects of flexibility of the superstructure, the peak top-deck acceleration and base-raft displacement are obtained by varying the superstructure time period for the single-story isolated structure, with and without impact conditions under the chosen earthquakes as shown in Figures 14, 15 and 16, respectively, for HDRB, LRB and the FPS with isolation parameters the same as before. The response is obtained for isolation gap distances $d_x = d_y = 4$ cm and 8 cm with a constant stiffness ratio $k_{xr} = k_{yr} = 5 \times 10^{-4}$ considering the torsionally uncoupled and coupled structures. It is seen from these figures that the superstructure acceleration continues to increase with the increase in time period of the superstructure, i.e. superstructure flexibility. In addition, the base-raft displacement shows a trend to marginally decrease with an increase in the fundamental time period of the

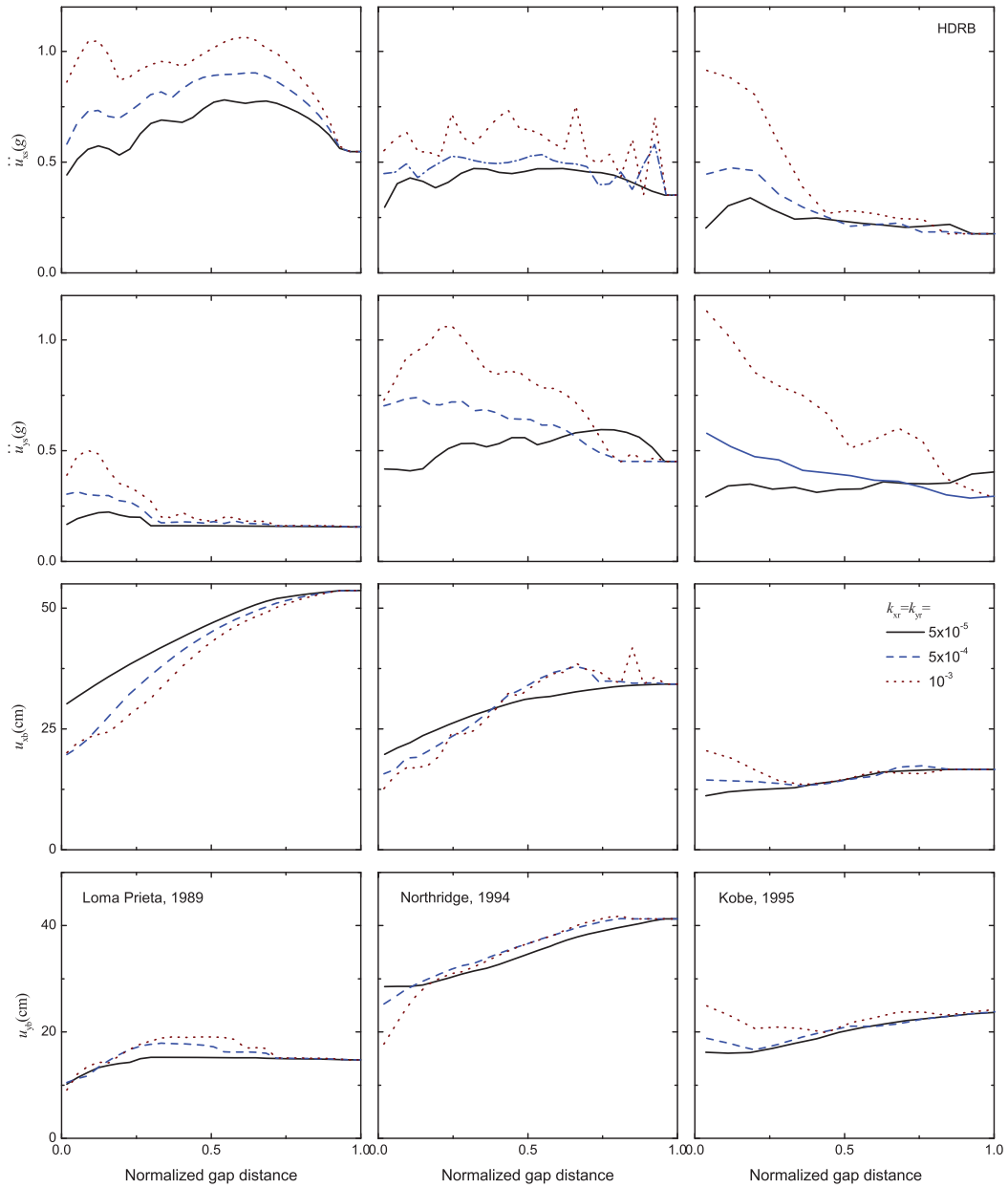

Figure 11. Effect of gap distances and stiffnesses of the adjacent structures on the response of base-isolated structures using HDRB under the Loma Prieta 1989, Northridge 1994 and Kobe 1995 earthquakes ($T_b = 2$ s and $\beta_{eff} = 0.1$).

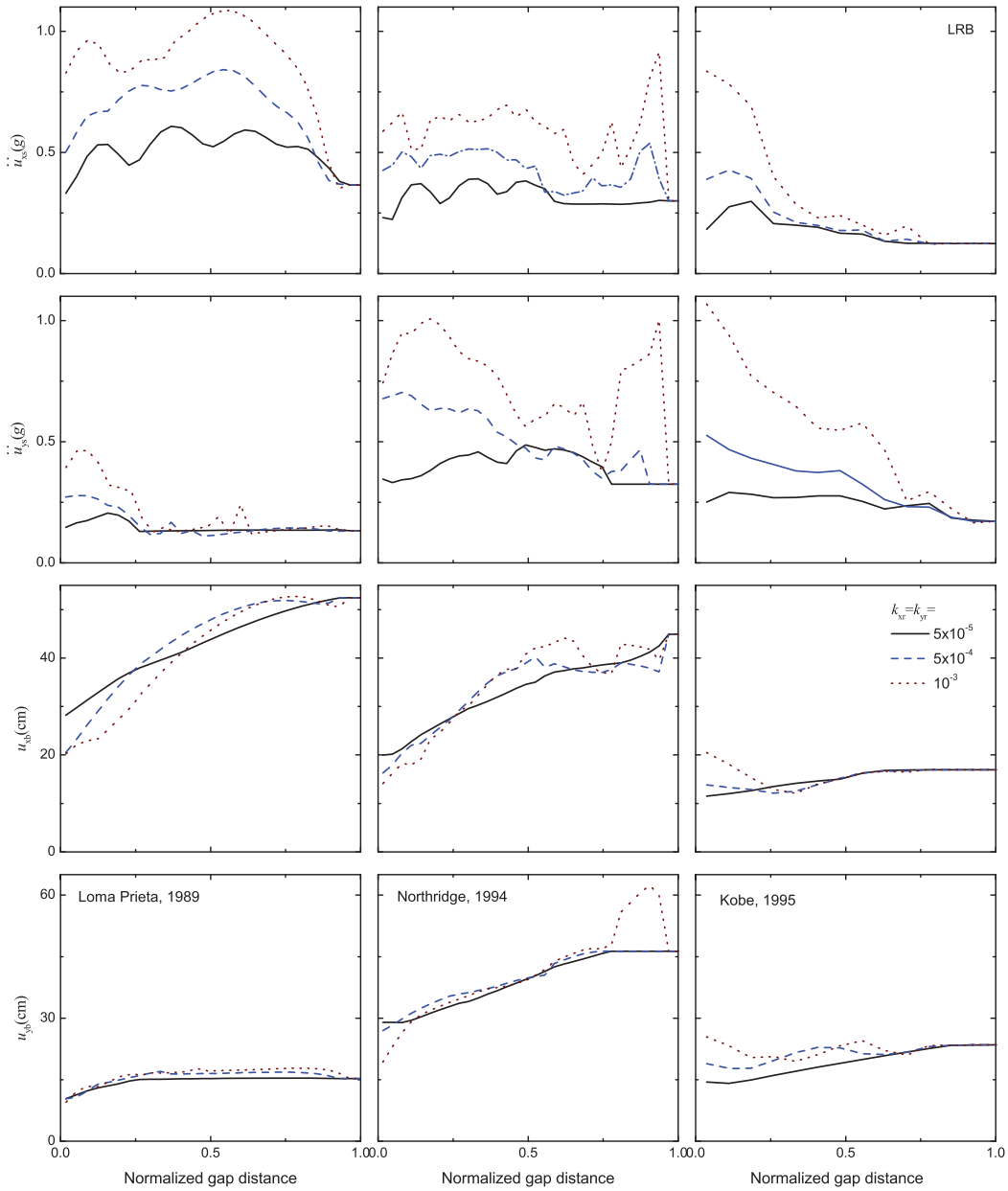

Figure 12. Effect of gap distances and stiffnesses of the adjacent structures on the response of base-isolated structures using LRB under the Loma Prieta 1989, Northridge 1994 and Kobe 1995 earthquakes ($T_b = 2.5$ s, $\xi_b = 0.05$, $q_j = 2.5$ cm and $f_{xj}^{y}/W = f_{yj}^{y}/W = 0.05$).

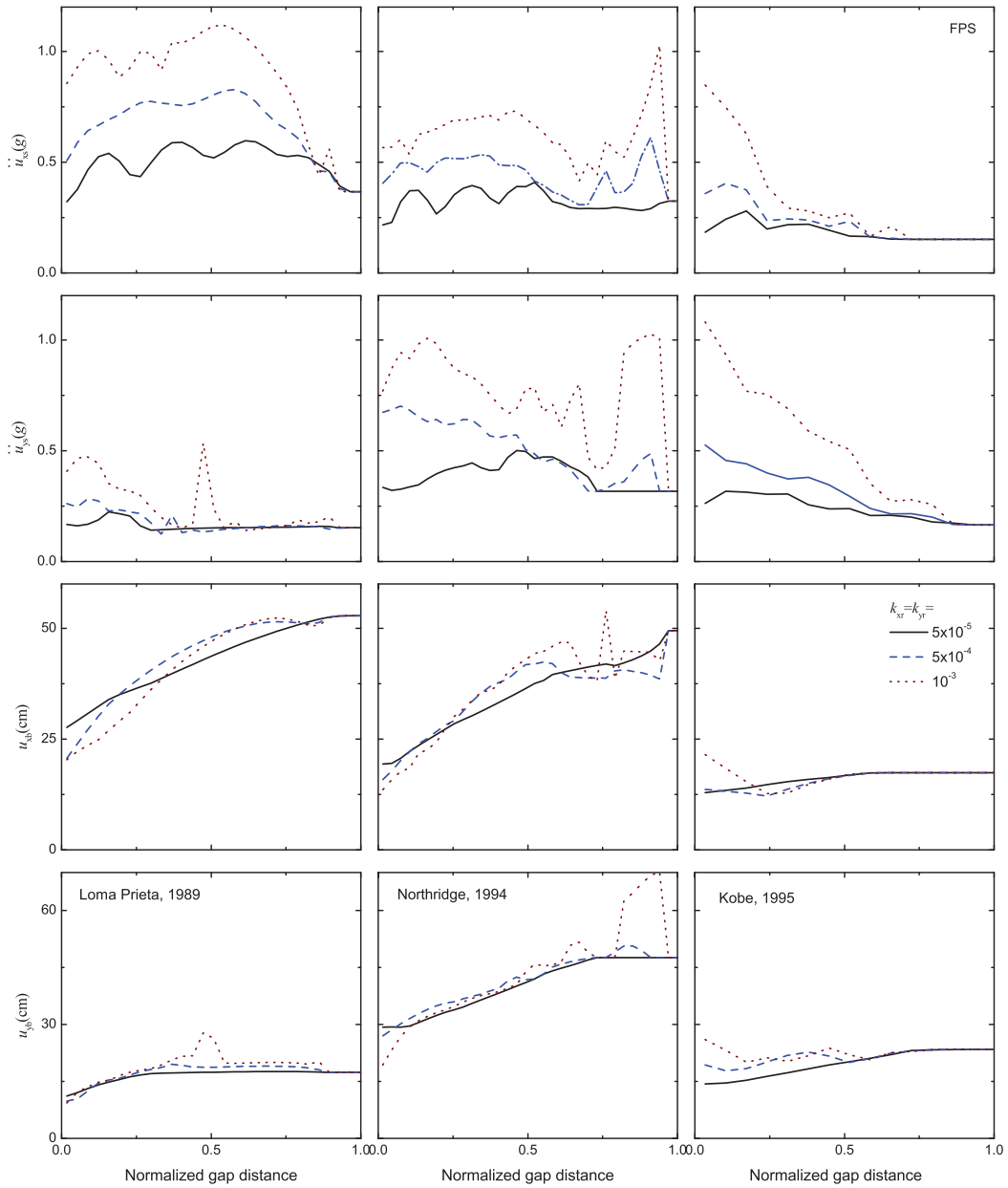

Figure 13. Effect of gap distances and stiffnesses of the adjacent structures on the response of base-isolated structures using the FPS under the Loma Prieta 1989, Northridge 1994 and Kobe 1995 earthquakes ($T_b = 2.5$ s, $\mu = 0.05$).

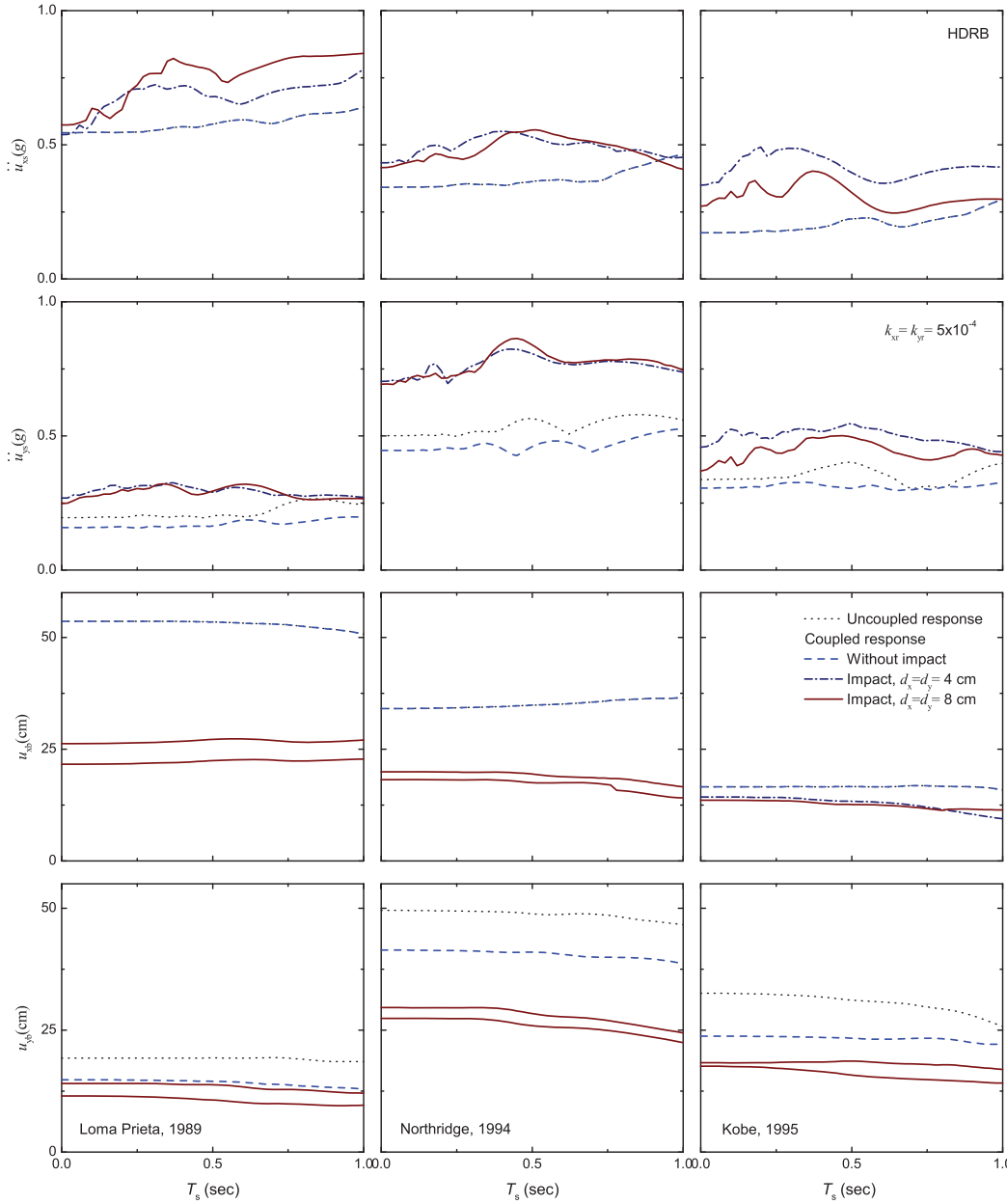

Figure 14. Effect of superstructure flexibility on the response of base-isolated structures using HDRB ($T_b = 2$ s and $\beta_{eff} = 0.1$) under the Loma Prieta, 1989, earthquake, $d_x = d_y = 4$ cm and $k_{xr} = k_{yr} = 5 \times 10^{-4}$.

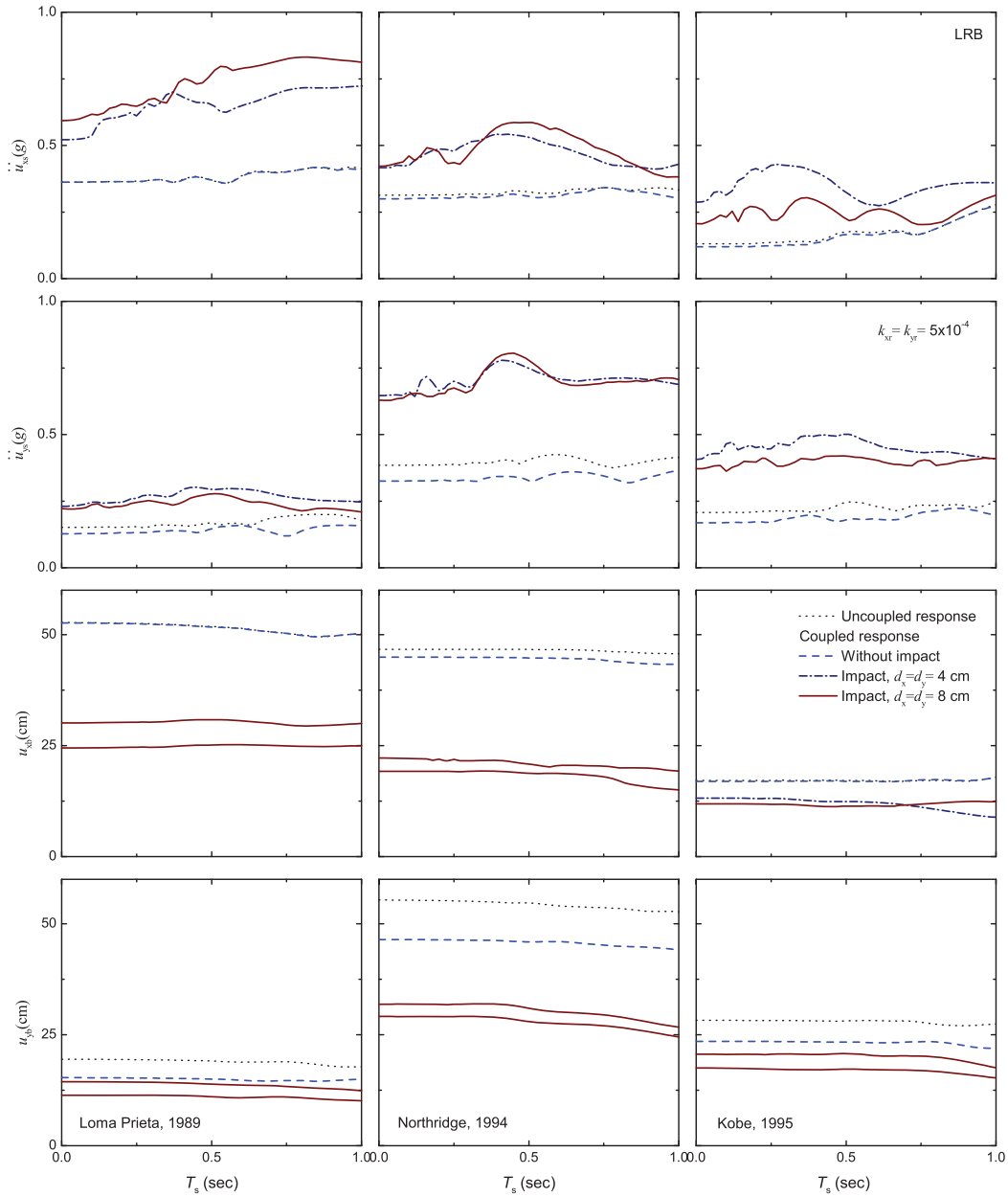

Figure 15. Effect of superstructure flexibility on the response of base-isolated structures using LRB ($T_b = 2.5$ s, $\xi_b = 0.05$, $q_j = 2.5$ cm and $f_{xj}^y/W = f_{yj}^y/W = 0.05$) under the Loma Prieta, 1989, earthquake, $d_x = d_y = 4$ cm and $k_{xr} = k_{yr} = 5 \times 10^{-4}$.

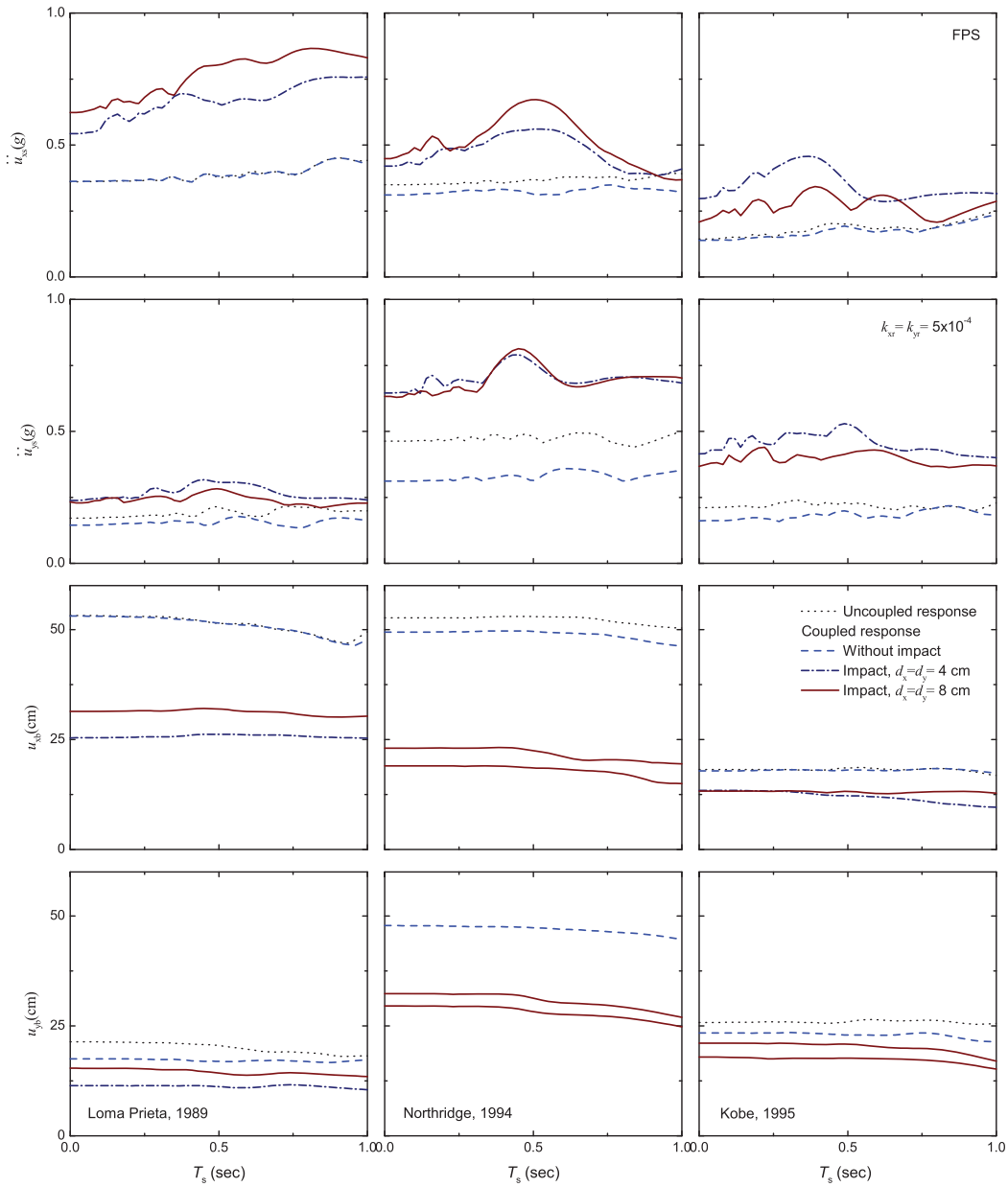

Figure 16. Effect of superstructure flexibility on the response of base-isolated structures using the FPS ($T_b = 2.5$ s and $\mu = 0.05$) under the Loma Prieta, 1989, earthquake, $d_x = d_y = 4$ cm and $k_{xr} = k_{yr} = 5 \times 10^{-4}$.

superstructure. However, the reduction in base-raft displacement is negligible. This implies that the behavior of the isolated structure during impact becomes adverse with increased superstructure flexibility.

6. CONCLUSIONS

The seismic response of the asymmetric base-isolated structure during impact with adjacent structures is investigated. The performance of different isolation systems during impact conditions is studied under real earthquake ground motions, in torsionally coupled and uncoupled cases. Parametric studies are conducted to observe the influence of different parameters of asymmetric base-isolated structures, such as eccentricities and flexibility of the superstructure, on the impact response. In addition, the effects of properties of adjacent structures such as stiffness and gap distances on the impact behavior are investigated. From the trend of the results of the present study the following conclusions can be drawn:

1. The dissimilarity in the isolator properties such as isolation stiffness and/or yield strength leads to torsional coupling in the response of the base-isolated structure and this alters the response significantly.
2. With the increasing torsional coupling, the impact response increases, and therefore it is mandatory to incorporate 3D analysis into the investigations. The torsionally coupled seismic response becomes adverse with increasing eccentricities.
3. The superstructure acceleration in the base-isolated structure increases significantly due to its impact upon the adjacent structures during earthquakes. Higher modes of vibration are excited when impact between the base-isolated structure and the adjacent structures occurs. The base-raft displacements are reduced consequently.
4. Superstructure acceleration in the isolated structure with impact phenomena is, in general, found to be less than the corresponding acceleration of a nonisolated structure implying that the benefits of isolation are preserved even with impact conditions.
5. As the gap distance between the base-isolated structure and the adjacent structures increases, there is an increase in the superstructure acceleration initially up to a certain value of the gap distance and then the superstructure acceleration decreases. Base-raft displacement increases with increase in gap distances.
6. The stiffness of the adjacent structures has significant influence on the response of the base-isolated structure during impact. The top-deck acceleration increases significantly with impact on stiffer adjacent structures.
7. Increased flexibility of the superstructure increases the superstructure acceleration during impact with the adjacent structure whereas base-raft displacement is reduced marginally with increased flexibility.

REFERENCES

American Association of State Highway and Transportation Officials (AASHTO), 1999, *Guide Specifications for Seismic Isolation Design*, Washington, D.C.

Anagnostopoulos, S. A., 1988, "Pounding of buildings in series during earthquakes," *Earthquake Engineering and Structural Dynamics* **16(3)**, 443–456.

Anagnostopoulos, S. A., 2004, "Equivalent viscous damping for modeling inelastic impacts in earthquake pounding problems," *Earthquake Engineering and Structural Dynamics* **33(8)**, 897–902.

Anagnostopoulos, S. A. and Spiliopoulos, K., 1992, "Investigation of earthquake induced pounding between adjacent buildings," *Earthquake Engineering and Structural Dynamics* **21(4)**, 289–302.

Buckle, I. G. and Mayes, R. L., 1990, "Seismic isolation, history, application and performance- a world view," *Earthquake Spectra* **6(2)**, 161–201.

Building Seismic Safety Council (BSSC), 1997, *NEHRP Guidelines for the Seismic Rehabilitation of Buildings*, FEMA-273 and Commentary FEMA-274, Federal Emergency Management Agency, Washington, D.C.

Davis, R. O., 1992, "Pounding of buildings modeled by an impact oscillator," *Earthquake Engineering and Structural Dynamics* **21(3)**, 253–274.

Dimova, S. L., 2000, "Numerical problems in modeling of collision in sliding systems subjected to seismic excitations," *Advances in Engineering Software* **31(7)**, 467–471.

Hall, J. F., Heaton, T. H., Halling, M. W., and Wald, D. J., 1995, "Near-source ground motion and its effects on flexible buildings," *Earthquake Spectra* **11(4)**, 569–605.

Jangid, R. S., and Datta, T. K., 1995, "Seismic behavior of base-isolated buildings: a state-of-the-art review," *Structures and Buildings* **110(2)**, 186–203.

Kelly, J. M., 1986, "Aseismic base isolation: review and bibliography," *Soil Dynamics and Earthquake Engineering* **5(4)**, 202–216.

Kikuchi, M. and Aiken, I. D., 1997, "An analytical hysteresis model for elastomeric seismic isolation bearings," *Earthquake Engineering and Structural Dynamics* **26(2)**, 215–231.

Koo, G. H., Lee, J. H., Yoo, B., and Ohtori, Y., 1999, "Evaluation of laminated rubber bearings for seismic isolation using modified macro-model with parameter equations of instantaneous apparent shear modulus," *Engineering Structures* **21(7)**, 594–602.

Maison, B. F. and Ventura, C. E., 1992, "Seismic analysis of base-isolated San Bernardino County building," *Earthquake Spectra* **8(4)**, 605–633.

Malhotra, P. K., 1997, "Dynamics of seismic impacts in base-isolated buildings," *Earthquake Engineering and Structural Dynamics* **26(8)**, 797–813.

Matsagar, V. A. and Jangid, R. S., 2003, "Seismic response of base-isolated structures during impact with adjacent structures," *Engineering Structures* **25(10)**, 1311–1323.

Matsagar, V. A. and Jangid, R. S., 2004, "Influence of isolator characteristics on the response of base-isolated structures," *Engineering Structures* **26(12)**, 1735–1749.

Matsagar, V. A. and Jangid, R. S., 2005, "Base-isolated building with asymmetries due to the isolator parameters," *Advances in Structural Engineering* **8(6)**, 603–622.

Nagarajaiah, S. and Sun, X., 2001, "Base-isolated FCC building: Impact response in Northridge earthquake," *Journal of Structural Engineering* **127(9)**, 1063–1075.

Park, Y. J., Wen, Y. K., and Ang, A. H.-S., 1986, "Random vibration of hysteretic systems under bi-directional ground motions," *Earthquake Engineering and Structural Dynamics* **14(4)**, 543–557.

Robinson, W. H., 1982, "Lead-rubber hysteretic bearings suitable for protecting structures during earthquakes," *Earthquake Engineering and Structural Dynamics* **10(4)**, 593–604.

Ryan, K. L. and Chopra, A. K., 2004, "Estimation of seismic demands on isolators in asymmetric structures using non-linear analysis," *Earthquake Engineering and Structural Dynamics* **33(3)**, 395–418.

Skinner, R. I., Kelly, J. M., and Heine, A. J., 1975, "Hysteretic dampers for earthquake- resistant structures," *Earthquake Engineering and Structural Dynamics* **3(3)**, 287–296.

Tena-Colunga, A. and Gomez-Soberon, L., 2002, "Torsional response of base-isolated structures due to asymmetries in the superstructure," *Engineering Structures* **24(12)**, 1587–1599.

Tsai, H.-C., 1997, "Dynamic analysis of base-isolated shear beams bumping against stops," *Earthquake Engineering and Structural Dynamics* **26(5)**, 515–528.

Tsopelas, P. C., Constantinou, M. C., and Reinhorn, A. M., 1991, "3D-BASIS-M: Non-linear dynamic analysis of multiple building base-isolated structures," Report No. NCEER-91-0014, National Center for Earthquake Engineering Research, University at Buffalo, Buffalo, NY.

Tsopelas, P. C., Nagarajaiah S., Constantinou, M. C. and Reinhorn A. M., 1994, "Non-linear dynamic analysis of multiple building base-isolated structures," *Computers & Structures* **50(1)**, 47–57.

Uniform Building Code (UBC), 1997, *International Conference of Building Officials*, Whittier, California.

Zayas, V. A., Low, S. S., and Mahin, S. A., 1990, "A simple pendulum technique for achieving seismic isolation," *Earthquake Spectra* **6(2)**, 317–333.